Interface enhancement of spin-polar phonon coupling in perovskite multiferroic superlattices

2012 EPL 100 17005

(http://iopscience.iop.org/0295-5075/100/1/17005)

A Letters Journal Exploring the Frontiers of Physics

October 2012

EPL, **100** (2012) 17005
doi: 10.1209/0295-5075/100/17005

www.epljournal.org

Interface enhancement of spin-polar phonon coupling in perovskite multiferroic superlattices

Hongwei Wang[1,2], Lixin He[1(a)] and Xifan Wu[2(b)]

[1] *Key Laboratory of Quantum Information, University of Science and Technology of China Hefei, Anhui, 230026, PRC*
[2] *Department of Physics and Institute for Computational Molecular Science, Temple University Philadelphia, PA 19122, USA*

received 3 August 2012; accepted in final form 7 September 2012
published online 15 October 2012

PACS 75.85.+t – Magnetoelectric effects, multiferroics
PACS 77.80.bn – Strain and interface effects
PACS 75.70.Cn – Magnetic properties of interfaces (multilayers, superlattices, heterostructures)

Abstract – First-principles calculations are carried out for $CaMnO_3/BaTiO_3$ short-period superlattices with epitaxial strain corresponding to growth on a $NdGaO_3$ substrate. The ferroelectricity and antiferrodistortion are analyzed under different magnetic orderings. It reveals that MnO_6 octohedral rotation is greatly suppressed at the interfaces, which effectively increases the spin-polar phonon coupling in $CaMnO_3$. Besides the conventional epitaxial-strain method, this mechanism provides an alternative way in engineering the spin-lattice coupling materials for an enhanced functionality.

Introduction. – The emergence of new phenomena at artificial heterostructure is currently at the center of scientific and technological interest [1–4]. Because a large variety of degrees of freedom such as spin, charge, structural orderings can be found in ABO_3 perovskite, it presents an ideal playground to explore the interactions among various orderings that could potentially lead to enhanced functionalities, and multifunctional materials [1].

Materials with large spin-polar phonon coupling belong to the above category and have recently attracted intense attention [5–9]. This is due to the potentially induced multiferrocity with large magnetostructural response resulting from the spin-lattice coupling, which is signified by the further softening of the polar phonon mode when these materials undergo transition from antiferromagnetic (AFM) phase to ferromagnetic (FM) phase [5–9]. Unfortunately the ground state of most known materials with large spin-lattice coupling are antiferromagnetic-paraelectric [5–9]. Thus, additional materials engineering is required in order to turn these materials into multiferroic phase for potential applications. Conventionally multiferroicity can be introduced by the mechanical boundary condition through the in-plane strain. The demonstration of epitaxial-strain–induced multiferroicity has been first established in $EuTiO_3$ by Fennie and Rabe [5], and later extended to $SrMnO_3$, $CaMnO_3$, etc. by the same group [6–8]. However one major challenge is that the required epitaxial strain could be large which makes it difficult for the experimental thin-film growth of the theoretically proposed materials [6–8].

On the other hand, the modern thin-film technology [2] allows the growth of superlattices (SLs) with sharp interfaces separating different constituent materials that may carry distinct instabilities originating from individual bulk materials [1,10–12]. In an earlier work, it has been shown by first-principles calculations that the antiferrodistortive (AFD) mode associated with oxygen octahedral rotation[1] and the ferroelectric (FE) polar mode can be in strong competition [11]. The suppression of the AFD mode at certain interfaces can actually favor the overall FE [11]. In a typical perovskite AMO_3 with large spin-lattice coupling, the spin ordering, FE and AFD are the three common instabilities. In the above, M is a

(a) E-mail: helx@ustc.edu.cn
(b) E-mail: xifanwu@temple.edu

[1] Here we adopt the notation that have been developed in ref. [12] in which rotation refers to the octahedral rotation around the [001] (out-of-plane) axis, while tilting refers to the octahedral rotation around the [110] (in-plane) axis.

magnetic atom with partially occupied *d*-orbitals and the so-called exchange angle (M-O-M bond angle) is crucial in controlling the magnetic interaction, which at the same time also strongly couples to both AFD and FE modes [13]. The couplings among spin, AFD and FE depend on the relative energetics of these instabilities. In bulk AMO_3, there is usually a strong AFD instability that suppresses the FE mode. Therefore an important question arises, could we have an interface mechanism in which the interface favors the spin-polar phonon coupling?

In this paper we show that the energetics of the AFD, FE and spin ordering can be drastically modified by interface engineering to favor the spin-polar phonon coupling. We take the $CaMnO_3$(CMO)/$BaTiO_3$ (BTO) SLs as our example systems. We find that the MnO_6 octahedral rotation will be strongly suppressed by the neighboring BaO layers, leading to a large enhancement of spin-polar phonon coupling. Taking the spontaneous polarization difference between G-AFM and FM phases as a measurement of spin-lattice coupling, we find it continuously increases with the increased density of interfaces while the relative CMO/BTO fraction is fixed at the same value. This clearly indicates the interface nature of the observed spin-lattice coupling enhancement. In order to have a better understanding microscopically, we develop an effective Hamiltonian model and show that an increased spin-lattice coupling will suppress the AFD which is consistent with our computational results.

Methods. – The calculations are based on the density functional (DFT) theory with spin-polarized generalized gradient approximation plus the on-site Coulomb interactions U (GGA + U) [14], The implemented in the Vienna *ab initio* simulations package (VASP) [15,16]. We adopt the Perdew-Burke-Ernzerhof functional revised for solids (PBEsol) [17]. The on-site Coulomb $U = 4.0\,\mathrm{eV}$ and exchange interaction $J = 0.88\,\mathrm{eV}$ are used for the Mn $3d$ electrons [18]. We use the plane-wave basis and projector augmented-wave pseudopotentials [19]. A 500 eV energy cutoff and $6 \times 6 \times 2$ k-point meshes converge the results very well. All ionic coordinates as well as the out-of-plane lattice constant are fully relaxed.

Results and discussion. – The ground state of orthorhombic (bulk) $CaMnO_3$ is G-type antiferromagnetic. The frequence of the polar mode is $\omega_{\mathrm{FE}} = 262\,\mathrm{cm}^{-1}$. Remarkably, the polar mode become unstable with $\omega_{\mathrm{FE}} = 40i\,\mathrm{cm}^{-1}$, in the FM state which is consistent with the large spin-polar phonon coupling found in this material [5–9]. It also has a large antiferrodistortive (AFD) instability associated to a non-polar oxygen rotational mode with an imaginary frequency $\omega_{\mathrm{AFD}} = 219i\,\mathrm{cm}^{-1}$ which is similar to previous theoretical results [20]. As a result, the octahedra rotates an angle about 8.94°. In contrast, $BaTiO_3$ is highly resistant to oxygen octahedral rotations and exhibits a robust FE state at room temperature.

The lattice mismatch between CMO (3.731 Å) and BTO (3.987 Å) is about 6.59%, which might be too large to grow high-quality CMO/BTO SLs. One may grow the CMO/BTO SLs on the $NdGaO_3$ substrate to reduce the lattice mismatch between CMO and BTO to the substrate to about ±3.37%. The alternation of compressive and tensile strains in the BTO and CMO layers induced by the substrate can effectively cancel out the mechanical tension and allow growing high-quality SLs [21]. We therefore fix the in-plane lattice constants of the SL to those of $NdGaO_3$ substrates (3.86 Å) in the calculations.

We first study the $(BaTiO_3)_1/(CaMnO_3)_1$ (1:1) and $(BaTiO_3)_2/(CaMnO_3)_2$ (2:2) SLs. To determine the ground-state spin structure, we calculate the total energies of a set of spin configurations (SCs) for the 1:1 and 2:2 SLs with full relaxations of the (electronic and lattice) structures. The results show that the stablest SCs are G-type AFM for 1:1, and A-type AFM for 2:2 SLs. The calculated magnetic moments of Mn ions are about $2.9\,\mu_B$, whereas Ti ions have negligible induced magnetic moments. We further fit the exchange integrals to a Heisenberg model $H = 1/2 \sum_{i,j} J_{ij} \mathbf{S}_i \cdot \mathbf{S}_j$, assuming nearest-neighbor coupling between the Mn ions. In the 1:1 SL, the intra-layer exchange interaction $J_{\mathrm{intra}} = -4.8\,\mathrm{meV}/\mu_B^2$, and the inter-layer exchange interaction $J_{\mathrm{inter}} = -0.86\,\mathrm{meV}/\mu_B^2$. In the 2:2 SL, the exchange interaction in the MnO_2 layer that sandwiched by the two CaO layer $J^{(1)}_{\mathrm{intra}} = 8.61\,\mathrm{meV}/\mu_B^2$, and in the MnO_2 layer that adjacent to the BaO layer $J^{(2)}_{\mathrm{intra}} = -1.11\,\mathrm{meV}/\mu_B^2$. The inter-layer exchange interaction $J^{(1)}_{\mathrm{inter}} = -24.54\,\mathrm{meV}/\mu_B^2$ and $J^{(2)}_{\mathrm{inter}} = -0.04\,\mathrm{meV}/\mu_B^2$, respectively. Here, the magnetic moments $\mathbf{S}$ are normalized to 1. The $J^{(2)}_{\mathrm{intra}}$ in the 2:2 SL is slightly frustrated. The Néel temperatures of the 1:1 and 2:2 SLs are 52 K and 59 K, respectively, calculated from Monte Carlo simulations [22].

Figures 1(a), (d) depict the local AFD associated with the TiO_6 or MnO_6 octahedral rotation in 1:1 and 2:2 SLs, respectively. Clearly, the MnO_6 octahedra that sandwiched between two CaO layers in 2:2 SL keeps a large rotation angle around 9° similar to that of the bulk value, and TiO_6 octahedra that sandwiched between two BaO layers has a rotation almost around 0°. This is consistent with the fact that CMO bulk has a strong AFD instability and BTO strongly resists the octahedra rotation. What is more intriguing, however, is the behavior of the interfacial layers of MnO_6 octahedra. Because of the presence of BaO on one side and CaO on the other side, MnO_6 at interface is exposed to a strongly broken mirror symmetry. As a result, this MnO_6 octahedron is found to have significantly reduced rotation angle which is around 2.0° in the 2:2 and 1:1 SLs in the G-type AFM state. The AFD rotations strongly depend on the spin configurations, and it is fully suppressed in the 1:1 SL in the FM state. Besides the AFD rotation, the MnO_6 octahedron also tilts around the [110] axis, as shown in fig. 1(b), (e) for the 1:1

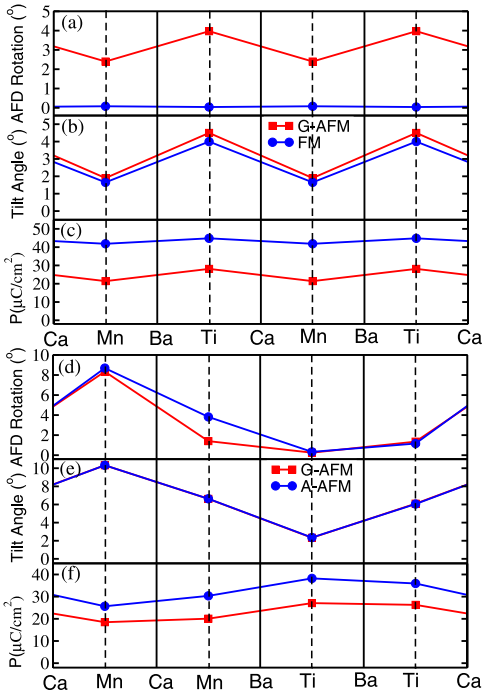

Fig. 1: (Color online) (a) The AFD rotations, (b) the octahedron tilting, and (c) the local electric polarization of the MnO_2 and TiO_2 layers in the 1:1 SL of the G-type AFM (red lines) and FM states (blue lines). (d) The AFD rotations, (e) the octahedron tilting, and (f) the local electric polarization of the MnO_2 and TiO_2 layers in the 2:2 SL of the G-type AFM (red lines) and A-type AFM states (blue lines). The results for FM state (not shown) are very close to those of the A-type AFM states.

and 2:2 SLs, respectively. The tilting angles show similar behavior as AFD angles. However, unlike the rotation, the tilting angles change little under different magnetic structures. And the reason will be discussed below. Because of the strong polarization in the $BaTiO_3$ layers, one may expect that the FE can also develop in the $CaMnO_3$ layer of the SL. We calculate the electric polarization using Berry phase formalism [23] for both 1:1 and 2:2 SLs in the G-type AFM state. Indeed, the SLs have spontaneous polarizations of $21.38\,\mu C/cm^2$ and $21.20\,\mu C/cm^2$, respectively, along the [001] direction. Since the SLs break the inversion symmetry resulting in a single-well potential, the spontaneous polarization will only develop in one direction [24]. There are also 5–$6\,\mu C/cm^2$ switchable polarizations developed along the [110] direction because of the octahedron rotation and titling as listed in table 1. To gain more insight, we calculate the layer polarization along [001] direction $p_z = \sum_i (e/\Omega) Z_i^* \lambda_i$ based on the linear approximation involving effective charges Z_i^* and small ionic distortions λ_i of each atoms i in the cell from a higher central symmetric non-polar reference structure. The effective charges are obtained from the cubic $CaMnO_3$ and $BaTiO_3$ phase by the finite-difference method. The resulting layer polarizations are presented in fig. 1. It can be seen that MnO_2-centered layers becomes polarized to almost the same degree of TiO_2-centered layers in both 1:1 and 2:2 SLs.

We now inspect the electric polarizations of SLs under various spin configurations. From table 1 it can be seen that all the BTO/CMO SLs undergo a large polarization increase when the spin configuration of the MnO_2 layer changes from antiferromagnetic (C-type or G-type AFM) to ferromagnetic (FM or A-type AFM). This is expected because of the large spin-lattice coupling in CMO, in which the FE phonon mode becomes softer when CMO undergoes a phase transition from AFM to FM. However as one of the most interesting results, this increase of polarization has a strong interface dependence. For the densest interface case, *i.e.*, 1:1 SL, the polarization change is also the largest and increases from about $21\,\mu C/cm^2$ to about $37\,\mu C/cm^2$. However with the decrease of interface density, the polarization increase becomes less and less drastic for which one can see that 2:2 SL changes from $21\,\mu C/cm^2$ to $32\,\mu C/cm^2$ and 3:3 SL changes from $24\,\mu C/cm^2$ to $33\,\mu C/cm^2$. One should note that the computational observed enhancement of spin-polar phonon coupling can originate from two sources of effect which are epitaxial strain and interface, respectively. In the present case, 1:1, 2:2, and 3:3 SLs all have the same volume fraction of BTO (50%) and CMO (50%), the most observed effect in 1:1 SL indicates that interface is essential for the enhancement of spin-polar phonon coupling.

What could be responsible for the enhancement of spin-polar phonon coupling? It is well known that the Mn-O-Mn exchange angle is essential in controlling the magnetic ordering [25]. However, the coupling between the FE modes and tilting modes through magnetic exchange energy is rather weak, because the tilting of octahedron would increase the Mn-O-Mn angle of one Mn-Mn pair, but decrease the angle of the other pair in the tilting plane, and the *average* Mn-O-Mn angle (thus, the exchange energy) change little to the octahedron tilting. To confirm this, we repeat the above first-principles calculations without allowing octahedron titling, and the obtained results are very similar. In contrast, the MnO_2 octahedral rotation and FE soft phonon modes can strongly couple to each other via the change of Mn-O-Mn angles. Indeed, at a closer inspection of what happens locally in the SLs, the drastic polarization change is found to be accompanied by an almost homogeneous increased layer polarization for both MnO_2-centered and TiO_2-centered layers in the 1:1 and 2:2 SLs and a suppression of the interfacial MnO_2 octahedral rotations relative to bulk material.

To illustrate why the interfacial octahedral rotation pinning effects would enhance the spin-polar phonon coupling in the 1:1 SL, we compare in fig. 2(a), (b), the change of the total energy as a function of the intra-layer exchange integral $J_{\rm intra}$ in bulk CMO and 1:1 SL, respectively. The intra-layer spin ordering can be continuously tuned from AFM($J_{\rm intra} < 0$) to FM($J_{\rm intra} > 0$)

Table 1: The electric polarization (in μC/cm^2) and energy (in meV/atom) in the $(BaTiO_3)_n/(CaMnO_3)_m$ (n:m) superlattices in different magnetic states.

		1:1	2:2	3:3	1:2	2:1
A-AFM	$P_{[001]}$	41.82	29.4	30.28	15.15	47.87
	$P_{[110]}$	$\sim$0	4.67	5.63	4.11	0
	Energy	-0.05	-0.69	-0.27	-0.7	-0.003
G-AFM	$P_{[001]}$	21.38	21.20	24.37	9.53	40.48
	$P_{[110]}$	6.74	5.42	6.60	5.18	0
	Energy	-0.27	0.14	0.67	-0.59	1.30
FM	$P_{[001]}$	36.79	31.92	33.42	19.45	47.87
	$P_{[110]}$	$\sim$0	2.76	4.79	1.32	0
	Energy	0	0	0	0	0

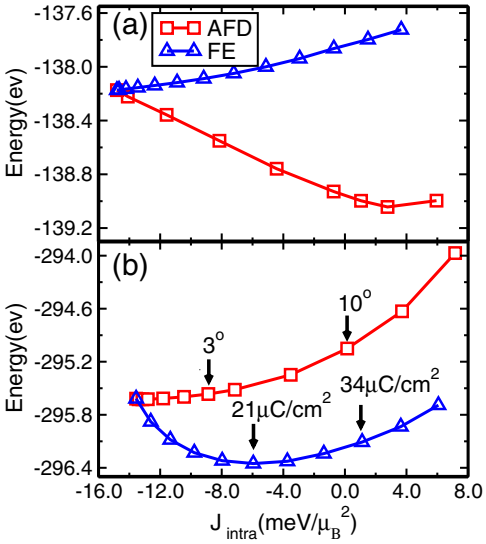

Fig. 2: (Color online) The total energies as functions of the MnO_2 intra-layer exchange energy $J_{\rm intra}$ for (a) bulk $CaMnO_3$ and (b) 1:1 SL through AFD rotation and FE modes. We also show the AFD rotation angle, and the polarization of the FE mode in the 1:1 SL.

by increasing either the MnO_2 octahedral rotation (red) or the amplitude of the FE soft phonon mode in both bulk $CaMnO_3$ and 1:1 SL. In bulk CMO, the intra-layer AFM-FM phase transition is realized by the increased octahedral rotation which has a much lower total energy than that of increased FE soft phonon mode. However in 1:1 SLs, the MnO_2 octahedral rotation is largely suppressed by the interface because it becomes energetically unfavorable (see fig. 2(b)). Therefore, the AFM-FM phase transition can be only driven by the increased FE soft phonon mode which results in the observed enhanced spin-polar phonon coupling.

To further understand how the the competition between the AFD and FE modes enhances the spin-polar phonon coupling in the 1:1 SL, we resort to a model Hamiltonian. For bulk $CaMnO_3$ in a uniform phase, the model Hamiltonian is

$$E(\{u_\Gamma, u_\varphi\}) = E_0 - \sum_{ij} J_{ij}(0)\mathbf{S}_i\cdot\mathbf{S}_j + \alpha u_\Gamma^2 + \beta u_\varphi^2 + \eta u_\Gamma^4 + \kappa u_\varphi^4 + \gamma u_\Gamma^2 u_\varphi^2, \quad (1)$$

where u_Γ and u_φ are the FE and AFD modes, respectively. The phonon frequencies $\alpha = \frac{1}{2}m_\Gamma\omega_\Gamma^2 - \sum_{ij}\frac{\partial^2 J_{ij}}{\partial^2 u_\Gamma}\mathbf{S}_i\cdot\mathbf{S}_j$ and $\beta = \frac{1}{2}m_\varphi\omega_\varphi^2 - \sum_{ij}\frac{\partial^2 J_{ij}}{\partial^2 u_\varphi}\mathbf{S}_i\cdot\mathbf{S}_j$ strongly depend on the spin configurations of the system. In bulk CMO, the FE mode has $\alpha>0$ in the G-type AFM states, and $\alpha<0$ in the FM state [5–9,26]. The anharmonic terms κ, η are positive. γ, which describes the coupling between the FE and AFD modes, is also positive. At the energy minima, we have $\partial E(\{u_\Gamma, u_\varphi\})/\partial u_\Gamma$=0, and $\partial E(\{u_\Gamma, u_\varphi\})/\partial u_\varphi$=0, *i.e.*,

$$\alpha u_\Gamma + 2\eta u_\Gamma^3 + \gamma u_\Gamma u_\varphi^2 = 0, \quad (2)$$

$$\beta u_\varphi + 2\kappa u_\varphi^3 + \gamma u_\varphi u_\Gamma^2 = 0. \quad (3)$$

It is easy to see from the equations that if $\alpha > 0$ ($\beta>0$), we have $u_\Gamma = 0 (u_\varphi = 0)$. The interesting cases are that both α and β are negative. When the coupling between the two modes is weak, *i.e.*, $\gamma < \gamma_c = \min(2\kappa\alpha/\beta, 2\eta\beta/\alpha)$, one has a solution that both u_Γ and u_φ are non-zero as schematically shown in fig. 3(a). However, when $\gamma > \gamma_c$, one has $u_\Gamma = 0$ and $u_\varphi^2 = -\beta/2\kappa$, if $\beta/2\kappa < \alpha/2\eta$, and u_φ=0 and $u_\Gamma^2 = -\alpha/2\eta$, if $\beta/2\kappa > \alpha/2\eta$, *i.e.*, one of the soft modes is fully suppressed[2] by the other mode that has stronger instability, because of the coupling between the two modes, as shown in fig. 3(b). The suppression of one mode enhances the amplitude of the other mode. This is exactly the case in the 1:1 SL. In bulk materials, the AFD mode is more unstable even in the FM state, therefore the FE mode is fully suppressed. In the 1:1 SL, when the MnO_2 intra-layer spin configuration is AFM, the AFD instability β is more negative than that of the FE mode despite of the interface effects, therefore, there are

[2]In the SLs, the FE mode would also couple to the electric polarization and the AFD mode would couple to the AFD modes in the adjacent layers, therefore, they would not be exactly zero.

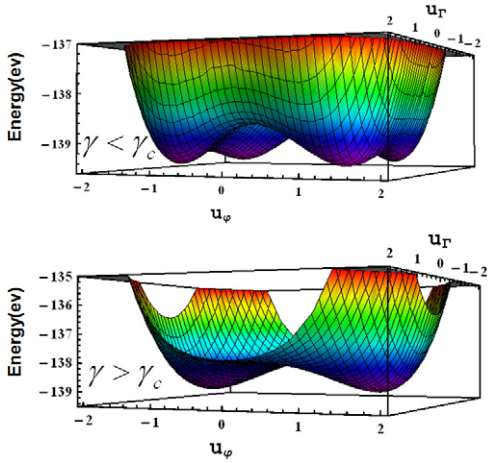

Fig. 3: (Color online) (a) The schematic shows the energy surfaces of the model Hamiltonian, eq. (1), in the case of (a) the coupling coefficient $\gamma < \gamma_c$ (weak coupling), and (b) the coupling coefficient $\gamma > \gamma_c$ (strong coupling), when both $\alpha < 0$, and $\beta < 0$.

significant AFD rotations, even though they are smaller than those in bulk CMO. However, when the MnO_2 intralayer spin configuration changes to FM, the FE mode becomes even more unstable than the AFD instability with the help of the BaO layer pinning effects to the AFD mode. Therefore, the AFD mode is fully suppressed. The suppression of the AFD mode greatly enhances the FE modes, resulting in the large spin-polar phonon coupling.

Summary and conclusions. – In conclusion, an interface mechanism in enhancing spin-polar phonon coupling is demonstrated by a first-principles computational method in $CaMnO_3/BaTiO_3$ systems. The key idea involved is that the MnO_2 octahedral rotation can be suppressed by the interfaces when the neighboring layer is constituted by BaO planes. As a result the Mn-O-Mn magnetic exchange angle, thus the magnetic ordering, is much more strongly coupled to the ferroelectric soft mode than to the AFD rotational mode. As a consequence it greatly increases the spin-polar phonon coupling in the material. Complementary to the conventional epitaxial-strain method, it provides a new way to further engineer spin-lattice coupling materials for enhanced magnetostructural and magetoelectric couplings. In experiments it can be realized and proven by the layer-by-layer epitaxial thin-films growth techniques.

* * *

The authors thanks X. X. Xi and Y. H. Chu for useful discussions. LH acknowledges the support from the Chinese National Fundamental Research Program 2011CB921200 and National Natural Science Funds for Distinguished Young Scholars. XW acknowledges the financial support of the start-up fund of Temple University and computational support by the National Science Foundation through TeraGrid resources provided by NICS under grant No. [TG-DMR120045].

REFERENCES

[1] Bousquet E. *et al.*, *Nature*, **452** (2008) 732.
[2] Lee H. N., Christen H. M., Chisholm M. F., Rouleau C. M. and Lowndes D. H., *Nature*, **433** (2005) 395.
[3] Ohtomo A. and Huang H. Y., *Nature*, **427** (2004) 423.
[4] Yu P. *et al.*, *Phys. Rev. Lett.*, **105** (2010) 027201.
[5] Fennie C. J. and Rabe K. M., *Phys. Rev. Lett.*, **97** (2006) 267602.
[6] Lee J. H. and Rabe K. M., *Phys. Rev. Lett.*, **104** (2010) 207204.
[7] Lee J. H. and Rabe K. M., *Phys. Rev. B*, **84** (2011) 104440.
[8] Lee J. H. and Rabe K. M., *Phys. Rev. Lett.*, **107** (2011) 067601.
[9] Hong J., Stroppa A., Íñiguez, Picozzi S. and Vanderbilt D., *Phys. Rev. B*, **85** (2012) 054417.
[10] Spaldin N. A., Cheong S. W. and Ramesh R., *Phys. Today*, **63** (2010) 38.
[11] Wu X., Rabe K. M. and Vanderbilt D., *Phys. Rev. B*, **83** (2011) 020104R.
[12] Zayak A. T., Huang X., Neaton J. B. and Rabe K. M., *Phys. Rev. B*, **74** (2006) 094104.
[13] Goodenough J. B., *Magnetism and the Chemical Bond* (John Wiley and Sons, New York, London) 1993.
[14] Anisimov V. I., Zaanen J. and Andersen O. K., *Phys. Rev. B*, **44** (1991) 943.
[15] Kresse G. and Hafner J., *Phys. Rev. B*, **47** (1993) R558.
[16] Kresse G. and Furthmuller J., *Phys. Rev. B*, **54** (1996) 11169.
[17] Perdew J. P., Ruzsinszky A., Csonka G. I., Vydrov O. A., Scuseria G. E., Constantin L. A., Zhou X. L. and Burke K., *Phys. Rev. Lett.*, **100** (2008) 136406.
[18] Liechtenstein A. I., Anisimov V. I. and Zaanen J., *Phys. Rev. B*, **52** (1995) 5467.
[19] Blochl P. E., *Phys. Rev. B*, **50** (1994) 17953.
[20] Bhattacharjee S., Bousquet E. and Ghosez P., *Phys. Rev. Lett.*, **102** (2009) 117602.
[21] Seo S. and Lee H. N., *Appl. Phys. Lett.*, **94** (2009) 232904.
[22] Cao K., Guo G.-C., Vanderbilt D. and He L., *Phys. Rev. Lett.*, **103** (2009) 257201.
[23] King-Smith R. D. and Vanderbilt D., *Phys. Rev. B*, **47** (1993) 1651.
[24] Sai N., Meyer B. and Vanderbilt D., *Phys. Rev. Lett.*, **84** (2000) 5636.
[25] Yamauchi K., Freimuth F., Blügel S. and Picozzi S., *Phys. Rev. B*, **78** (2008) 014403.
[26] Garcia-Fernandez P., Aramburu J. A. and Moreno M., *Phys. Rev. B*, **83** (2011) 174406.